Journal of Biomedical Optics

BiomedicalOptics.SPIEDigitalLibrary.org

Comparison of three light doses in the photodynamic treatment of actinic keratosis using mathematical modeling

Anne-Sophie Vignion-Dewalle
Nacim Betrouni
Jean-Baptiste Tylcz
Maximilien Vermandel
Laurent Mortier
Serge Mordon

SPIE.

Comparison of three light doses in the photodynamic treatment of actinic keratosis using mathematical modeling

Anne-Sophie Vignion-Dewalle,[a] Nacim Betrouni,[a,b,*] Jean-Baptiste Tylcz,[a] Maximilien Vermandel,[a,b,c] Laurent Mortier,[a,b] and Serge Mordon[a,b]
[a]INSERM, U1189, ONCO-THAI, 1, avenue Oscar Lambret, F-59037 Lille Cedex, France
[b]University of Lille Nord de France, 365 bis, rue Jules Guesde, BP 50458, F-59658 Villeneuve d'Ascq Cedex, France
[c]CHRU de Lille, Hôpital Huriez, Service Dermatologie, 2, avenue Oscar Lambret, France

Abstract. Photodynamic therapy (PDT) is an emerging treatment modality for various diseases, especially for cancer therapy. Although high efficacy is demonstrated for PDT using standardized protocols in nonhyperkeratotic actinic keratoses, alternative light doses expected to increase efficiency, to reduce adverse effects or to expand the use of PDT, are still being evaluated and refined. We propose a comparison of the three most common light doses in the treatment of actinic keratosis with 5-aminolevulinic acid PDT through mathematical modeling. The proposed model is based on an iterative procedure that involves determination of the local fluence rate, updating of the local optical properties, and estimation of the local damage induced by the therapy. This model was applied on a simplified skin sample model including an actinic keratosis lesion, with three different light doses (red light dose, 37 J/cm^2, 75 mW/cm^2, 500 s; blue light dose, 10 J/cm^2, 10 mW/cm^2, 1000 s; and daylight dose, 9000 s). Results analysis shows that the three studied light doses, although all efficient, lead to variable local damage. Defining reference damage enables the nonoptimal parameters for the current light doses to be refined and the treatment to be more suitable. [DOI: 10.1117/1.JBO.20.5.058001]

Keywords: photodynamic therapy; light doses comparison; protoporphyrin IX; mathematical modeling.

Paper 150032R received Jan. 21, 2015; accepted for publication Apr. 17, 2015; published online May 22, 2015.

1 Introduction

Photodynamic therapy (PDT) is an emerging cancer therapy combining light of an appropriate wavelength, a nontoxic photosensitizer, and sufficient molecular oxygen to generate reactive oxygen species and destroy tumors.[1,2] Many reports on PDT using 5-aminolevulinic acid (5-ALA-PDT)[3–7] have been published since the early work of Kennedy et al.[8] 5-ALA is a precursor of the heme biosynthesis and exogenous administration of 5-ALA leads to accumulation of the photosensitizer protoporphyrin IX (PpIX), preferentially in neoplastic tissues.[9] As it can be applied topically for dermatological indications, 5-ALA brings several benefits over other photosensitizers such as porphyrin derivatives, which have to be systemically applied.[7] In dermatology, PDT using 5-ALA or its methyl ester (MAL-PDT) has proven to be an efficient topical treatment for numerous (pre) malignant conditions[5,10] including actinic keratosis (AK),[7,11,12] Bowen's disease,[13,14] and superficial basal cell carcinoma.[15,16]

Several studies have reported that MAL-PDT with red light using a total light dose of 37 J/cm^2 and a fluence rate of 75 mW/cm^2 is an effective treatment option for AK and results in similar response rates and improved cosmetic outcomes compared with standard therapies.[12,17] However, with these light dose parameters, the treatment appears to be very painful[18,19] and concurrent use of cold air analgesia may be required to relieve discomfort and pain.[17,18] Recently, Apalla et al.[20] demonstrated that red light PDT using a fluence rate between 25 and 50 mW/cm^2 was as effective in the treatment of AK as using a fluence rate of 75 mW/cm^2, but much better tolerated by patients. When using blue light at a dose of 10 J/cm^2 delivered at a fluence rate of 10 mW/cm^2, topical ALA PDT has also been demonstrated to be a highly effective and safe treatment for multiple actinic keratoses of the face and scalp.[11,21] Finally, PDT of AK using daylight activation has proven to be as effective as and more manageable in clinical practice than conventional red light PDT.[22] With pain scores significantly reduced compared to conventional red light illumination, daylight exposure was also found to be better tolerated and more convenient for the patient.

Looking at these various light doses with similar efficiencies but variable tolerabilities, a mathematical modeling of the PDT process was clearly felt to be necessary to obtain a better understanding of the process and of the relationship between process parameters and process performance (in terms of efficiency and tolerability).[23–25] This better understanding should result in an improved determination of the optimal treatment parameters.[26,27]

In this paper, we propose to model the PDT process for AK treatment based on the study of Farrell et al.[28] and using a skin sample model resulting from the inclusion of an AK to the simplified skin model of Liu et al.[24] The proposed model involves

*Address all correspondence to: Nacim Betrouni, E-mail: nacim.betrouni@inserm.fr

1083-3668/2015/$25.00 © 2015 SPIE

an iterative procedure alternating between updating the local fluence rate and updating the PpIX absorption coefficient. The local fluence rate is calculated by solving the one-dimensional diffusion equation [28,29] while the PpIX absorption coefficient is estimated considering biological elimination and continuous accumulation of the PpIX in the AK as well as photobleaching. Standard models are used for biological elimination and continuous accumulation whereas an original simplified model based on an unlimited availability of oxygen and depending both on the local fluence rate and the incident wavelengths is proposed for photobleaching. Finally, a photodynamic dose defined as a function of the singlet oxygen molecules generated during the treatment is used to quantify the local damage induced by PDT.

The proposed model was applied with the three most common light doses for PDT of AK:

1. Dose 1: red light dose, 632 nm, 37 J/cm^2, 75 mW/cm^2, 500 s;[30,31]
2. Dose 2: blue light dose, 417 nm, 10 J/cm^2, 10 mW/cm^2, 1000 s;[32,33]
3. Dose 3: daylight dose, the fluence rate for the daylight was set to the solar spectral irradiance downloaded from Ref. 34 (this fluence rate was consistent with the one used in Campbell et al.[35]), 9000 s;[22]

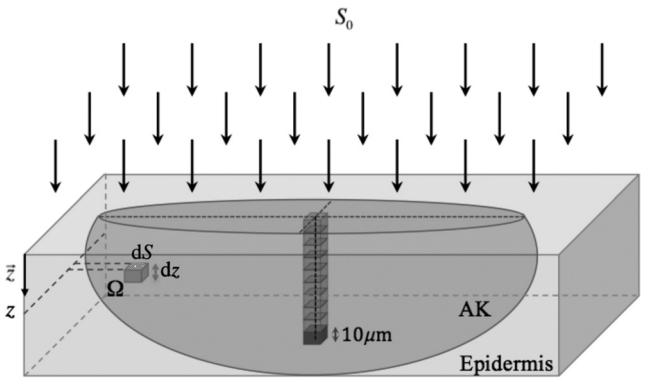

Fig. 1 Representation of the skin sample model perpendicularly irradiated by a planar beam S_0. The sampling of the skin sample model is partially illustrated and the deepest point of the AK is identified as the darkest cuboid of the central stack of cuboids.

Analysis of the resulting photodynamic doses allowed for a comparison of the doses in terms of local damages and the determination of a reference local damage, defined as the minimum of the three local damages obtained at the deepest part of the actinic keratosis sample. Then it allowed for the estimation of the treatment times required with the fluence rates of the three above-mentioned light doses to achieve this reference damage in the deepest part of the actinic keratosis sample.

2 Material

2.1 *Skin Sample Model*

As AKs are confined to the epidermis (the basement membrane is intact), the simplified skin sample model we used consists of an epidermis section with a thickness of 100 μm[24] including an AK, designed as an ellipsoid. The epidermis and AK tissues are both assumed to be homogeneous. To account for the thickening of the epidermis generally observed in AK, the diameter in depth of the ellipsoid is set to 150 μm. According to the curettage usually performed prior to PDT, the skin sample model displayed on Fig. 1 is finally assumed.

A primary planar beam with fluence rate S_0 is assumed to perpendicularly irradiate the surface of the skin sample model (Fig. 1).

Let $\vec{z}$ be the beam direction, which is also the depth direction of the skin sample model.

Let Ω be a cuboid with base surface dS and depth dz, located at depth z in the AK (Fig. 1).

2.2 *Light Doses*

Three effective light doses as reported in literature[22,30–33] and with parameters summarized in Table 1 are studied.

Usual 3-h and 30-min incubations with 5-ALA under occlusive dressing are assumed for the red and blue light doses and for the daylight dose, respectively.

3 Method

3.1 *Local Total Fluence Rate Determination*

The local total fluence rate, φ, at location $\vec{r}$ in the skin sample model, is given by the sum of the local diffuse fluence rate, φ_d, and the local incident fluence rate, φ_i [Eq. (1)]

Table 1 Description of the three light doses.

	Red light dose	Blue light dose	Daylight dose
References	Moseley et al.[30] Tyrrell et al.[31]	DUSA Pharmaceuticals[32] Warren et al.[33]	Wiegell et al.[22]
Fluence rate spectrum	Gaussian distribution. Mean: 632 nm FWHM: 19 nm	Gaussian distribution. Mean: 417 nm FWHM: 30 nm	Solar emission spectrum. Downloaded from Ref. 34. Consistent with Campbell et al.[35]
Fluence	37 J/cm^2	10 J/cm^2	
Exposure time	500 s	1000 s	9000 s
Fluence rate	75 mW/cm^2	10 mW/cm^2	

$$\varphi(\vec{r}) = \phi_d(\vec{r}) + \varphi_i(\vec{r}). \quad (1)$$

Due to both the biological elimination of PpIX, the conversion of 5-ALA into PpIX and the photobleaching, the PpIX absorption coefficient and, therefore, the local total fluence rate change during treatment. Similarly to Farrell et al.[28] based on a PpIX concentration varying only with depth, z, below the irradiated surface, we have deduced Eq. (2) from Eq. (1)

$$\varphi(z) = \varphi_d(z) + \varphi_i(z). \quad (2)$$

From Farrell et al.[28] and Carp et al.,[29] the local diffuse fluence rate, φ_d, can be expressed using Eq. (3),

$$\phi_d(z) = S_0\left\{\frac{b}{\sqrt{\mu_{\text{eff}}(z)}}\exp\left[-\int_0^z \mu_{\text{eff}}(w)\mathrm{d}w\right] + P(z)\exp\left[-\int_0^z \mu_t'(w)\mathrm{d}w\right]\right\}, \quad (3)$$

where

- The total absorption coefficient, μ_a, is the sum of the actinic keratosis absorption coefficient, $\mu_{a,\text{AK}}$, and the PpIX absorption coefficient, $\mu_{a,\text{PpIX}}$,
- The total transport coefficient, μ_t', is the sum of the total absorption coefficient, μ_a, and the actinic keratosis reduced scattering coefficient, $\mu_{s,\text{AK}}'$,
- The effective attenuation coefficient, μ_{eff}, is defined as $\sqrt{3\mu_a(z)\mu_t'(z)}$,
- The two parameters, b and $P(z)$, depending on both the optical properties of the actinic keratosis and the boundary conditions at the actinic keratosis surface, are computed as described in Farrell et al.[28]

For a planar beam irradiation, the local incident fluence rate, φ_i, is written in the form of Eq. (4),[28,29]

$$\phi_t(z) = S_0\exp\left[-\int_0^z \mu_t'(w)\mathrm{d}w\right]. \quad (4)$$

3.2 Evolution of the Protoporphyrin IX Absorption Coefficient

Because the three different above mentioned processes affect the PpIX absorption coefficient, the change in the number of PpIX molecules can be expressed as follows:

$$\frac{\mathrm{d}M_{\text{PpIX}}(t,z)}{\mathrm{d}t} = -M_{\text{PpIX},b}(t,z) + M_{\text{PpIX},c}(t,z) - M_{\text{PpIX},p}(t,z), \quad (5)$$

where

- $M_{\text{PpIX}}(t,z)$ is the number of PpIX molecules contained in Ω at time t,
- $M_{\text{PpIX},b}(t,z)$, $M_{\text{PpIX},c}(t,z)$, and $M_{\text{PpIX},p}(t,z)$ are the number of PpIX molecules biologically eliminated, generated by conversion from 5-ALA, and eliminated by photobleaching, respectively, at time t.

3.2.1 Biological elimination of protoporphyrin IX

The biological elimination of PpIX leads to an exponential decay of the number of PpIX molecules such that $M_{\text{PpIX},b}(t,z)$ can be expressed through Eq. (6),

$$M_{\text{PpIX},b}(t,z) = \frac{M_{\text{PpIX}}(t,z)}{\tau_b}, \quad (6)$$

where τ_b is the time constant for the biological elimination of PpIX for actinic keratosis.

3.2.2 Conversion of 5-aminolevulinic acid into protoporphyrin IX

To model the conversion of 5-ALA into PpIX, we use the fluorescence data reported in Wiegell et al.[22] These data, measured from actinic keratosis within 3 h incubation after MAL application, suggest an exponential increase with time of the number of PpIX molecules leading to Eq. (7)

$$M_{\text{PpIX},c}(t,z) = \frac{M_{\text{PpIX}}(t,z)}{\tau_c}, \quad (7)$$

where τ_c is the time constant for the conversion of 5-ALA into PpIX.

3.2.3 Photobleaching

As shown by Dysart et al.,[36] the change in the concentration of PpIX molecules due to the singlet oxygen-mediated photobleaching can be expressed by a differential equation. This differential equation can be written in terms of the number of PpIX molecules, $M_{\text{PpIX}}(t,z)$

$$M_{\text{PpIX},p}(t,z) = \frac{\kappa}{\aleph \times \mathrm{d}S \times \mathrm{d}z} \times M_{\text{PpIX}}(t,z) \times M_{^1O}(t,z), \quad (8)$$

where

- κ is the bimolecular rate constant for the reaction of singlet oxygen with PpIX,
- $\aleph$ is the Avogadro number,
- $M_{^1O}(t,z)$ is the number of singlet oxygen molecules contained in Ω at time t.

The change in the number of singlet oxygen molecules contained in Ω at time t can be expressed as [Eq. (9)]:

$$\frac{\mathrm{d}M_{^1O}(t,z)}{\mathrm{d}t} = +M_{^1O}^{+}(t,z) - M_{^1O}^{-}(t,z), \quad (9)$$

where

- $M_{^1O}^{+}(t,z)$ is the number of PpIX molecules generated in Ω at time t when the PpIX molecules, excited by the absorption of photons, return to the ground state,
- $M_{^1O}^{-}(t,z)$ is the number of PpIX molecules consumed in Ω at time t.

Using the first-order approximation of the derivative, Eq. (10) is obtained:

$$M_{^1O}(t,z) = M_{^1O}(t-\mathrm{d}t,z) + dt \times M^{+}_{^1O}(t,z) - \mathrm{d}t \times M^{-}_{^1O}(t,z). \tag{10}$$

According to the short lifetimes of the excited states of the PpIX (~nanoseconds), simultaneity between the absorption of a photon and the subsequent production of singlet oxygen molecules is assumed such that $M^{+}_{^1O}(t,z)$ can be estimated as follows:

$$M^{+}_{^1O}(t,z) = \int_{\tilde{\lambda}} \left\{ \gamma_{\tilde{\lambda}} \times \frac{\varphi(t,z,\tilde{\lambda}) \times \mathrm{d}S}{E_{\tilde{\lambda}}} \times \mu_{a,\mathrm{PpIX}}(t,z,\tilde{\lambda}) \times \mathrm{d}z \right\} d\tilde{\lambda}, \tag{11}$$

where

- The (dimensionless) singlet oxygen quantum yield, $\gamma_{\tilde{\lambda}}$, is the number of singlet oxygen molecules generated for each photon of wavelength $\tilde{\lambda}$ absorbed by a PpIX molecule when the PDT process is not limited by the availability of oxygen concentration,
- Computed from the local total fluence rate reaching $\mathrm{d}S$ at time t, $\varphi(t,z,\tilde{\lambda})$, and from the energy of a photon of wavelength $\tilde{\lambda}$, $E_{\tilde{\lambda}}$, the term $\phi(t,z,\tilde{\lambda}) \times \mathrm{d}S / E_{\tilde{\lambda}}$ represents the number of photons of wavelength λ reaching $\mathrm{d}S$ per unit of time.

Moreover, regarding the short singlet oxygen lifetime in biological media (~hundredths of microseconds[36]) compared to the interval of time $\mathrm{d}t$ usually used for computations (~hundred microseconds), all the singlet oxygen molecules present in Ω at time $t-\mathrm{d}t$, $M_{^1O}(t-\mathrm{d}t,z)$, are assumed to be consumed during dt such that $M^{-}_{^1O}(t,z)$ can be approximated by $M_{^1O}(t-\mathrm{d}t,z)/\mathrm{d}t$ leading to Eq. (12),

$$M_{^1O}(t,z) = \mathrm{d}t \times M^{+}_{^1O}(t,z) = \mathrm{d}t \times \int_{\tilde{\lambda}} \left\{ \gamma_{\tilde{\lambda}} \times \frac{\phi(t,z,\tilde{\lambda}) \times \mathrm{d}S}{E_{\tilde{\lambda}}} \times \mu_{a,\mathrm{PpIX}}(t,z,\tilde{\lambda}) \times \mathrm{d}z \right\} \mathrm{d}\tilde{\lambda}. \tag{12}$$

Finally, the number of PpIX molecules eliminated by photobleaching can be obtained through Eq. (13),

$$\begin{aligned} M_{\mathrm{PpIX},p}(t,z) &= \frac{\kappa}{\aleph \times \mathrm{d}S \times \mathrm{d}z} \times M_{\mathrm{PpIX}}(t,z) \times \mathrm{d}t \\ &\times \int_{\tilde{\lambda}} \left\{ \gamma_{\tilde{\lambda}} \times \frac{\phi(t,z,\tilde{\lambda}) \times \mathrm{d}S}{E_{\tilde{\lambda}}} \times \mu_{a,\mathrm{PpIX}}(t,z,\tilde{\lambda}) \times \mathrm{d}z \right\} \mathrm{d}\tilde{\lambda} \\ &= \frac{\kappa}{\aleph} \times M_{\mathrm{PpIX}}(t,z) \times \mathrm{d}t \\ &\times \int_{\tilde{\lambda}} \left\{ \gamma_{\tilde{\lambda}} \times \frac{\phi(t,z,\tilde{\lambda})}{E_{\tilde{\lambda}}} \times \mu_{a,\mathrm{PpIX}}(t,z,\tilde{\lambda}) \right\} \mathrm{d}\tilde{\lambda}. \end{aligned} \tag{13}$$

3.2.4 *Overall evolution*

Inserting Eqs. (6), (7), and (13) into Eq. (5) gives Eq. (14)

$$\frac{\mathrm{d}M_{\mathrm{PpIX}}(t,z)}{\mathrm{d}t} = M_{\mathrm{PpIX}}(t,z) \times \left\{ -\frac{1}{\tau_b} + \frac{1}{\tau_c} - \frac{\kappa}{\aleph} \times \mathrm{d}t \times \int_{\tilde{\lambda}} \left\{ \gamma_{\tilde{\lambda}} \times \frac{\phi(t,z,\tilde{\lambda})}{E_{\tilde{\lambda}}} \times \mu_{a,\mathrm{PpIX}}(t,z,\tilde{\lambda}) \right\} \mathrm{d}\tilde{\lambda} \right\}. \tag{14}$$

Based on the relation $\mu_{a,\mathrm{PpIX}}(t,z,\lambda) = \varepsilon_{\mathrm{PpIX}}(\lambda) \times C_{\mathrm{PpIX}}(t,z) = \varepsilon_{\mathrm{PpIX}}(\lambda) \times M_{\mathrm{PpIX}}(t,z)/(\aleph \times \mathrm{d}S \times \mathrm{d}z)$, where $\varepsilon_{\mathrm{PpIX}}(\lambda)$ and $C_{\mathrm{PpIX}}(t,z)$ are the PpIX molar extinction coefficient for wavelength λ and the PpIX concentration at depth z and time t, respectively, Eq. (14) leads to Eq. (15),

$$\frac{\mathrm{d}\mu_{a,\mathrm{PpIX}}(t,z,\lambda)}{\mathrm{d}t} = \mu_{a,\mathrm{PpIX}}(t,z,\lambda) \times \left\{ -\frac{1}{\tau_b} + \frac{1}{\tau_c} - \frac{\kappa}{\aleph} \times \mathrm{d}t \times \int_{\tilde{\lambda}} \left\{ \gamma_{\tilde{\lambda}} \times \frac{\phi(t,z,\tilde{\lambda})}{E_{\tilde{\lambda}}} \times \mu_{a,\mathrm{PpIX}}(t,z,\tilde{\lambda}) \right\} \mathrm{d}\tilde{\lambda} \right\}. \tag{15}$$

3.3 *Photodynamic Dose*

Because damage induced by PDT is a result of the generation of singlet oxygen, the photodynamic dose can be defined as the total cumulative singlet oxygen produced during treatment time, denoted T. From Eq. (11), it follows:

$$\begin{aligned} \mathrm{PD}(z) &= \int_0^T M^{+}_{^1O}(t,z)\mathrm{d}t \\ &= \int_0^T \int_{\tilde{\lambda}} \left\{ \gamma_{\tilde{\lambda}} \times \frac{\phi(t,z,\tilde{\lambda}) \times \mathrm{d}S}{E_{\tilde{\lambda}}} \times \mu_{a,\mathrm{PpIX}}(t,z,\tilde{\lambda}) \times \mathrm{d}z \right\} \mathrm{d}\tilde{\lambda}\mathrm{d}t. \end{aligned} \tag{16}$$

Using the sampling times $\{t_i = i \times \mathrm{d}t\}_{0 \le t_i \le T}$, $\mathrm{PD}(z)$ can be approximated as in Eq. (17)

$$\mathrm{PD}(z) \approx \sum_{t_i} \left\{ \mathrm{d}t \times \int_{\tilde{\lambda}} \left\{ \gamma_{\tilde{\lambda}} \times \frac{\phi(t_i,z,\tilde{\lambda}) \times \mathrm{d}S}{E_{\tilde{\lambda}}} \times \mu_{a,\mathrm{PpIX}}(t_i,z,\tilde{\lambda}) \times \mathrm{d}z \right\} \mathrm{d}\tilde{\lambda} \right\}. \tag{17}$$

Thus, the calculation of $\mathrm{PD}(z)$ requires the determination of both the PpIX absorption coefficient and the local total fluence rate as treatment progresses.

Assuming an initial PpIX absorption coefficient, $\mu_{a,\mathrm{PpIX}}(0,z,\lambda)$, the initial local total fluence rate, $\varphi(0,z,\lambda)$, at any point of the skin model (Fig. 1) can be calculated from Eqs. (2)–(4). The PpIX absorption coefficient at time $t_1 = \mathrm{d}t$ can then be obtained considering the following approximation of Eq. (15)

$$\begin{aligned} \mu_{a,\mathrm{PpIX}}(t+\mathrm{d}t,z,\lambda) = \; & \mu_{a,\mathrm{PpIX}}(t,z,\lambda) + \mathrm{d}t \times \mu_{a,\mathrm{PpIX}}(t,z,\lambda) \\ & \times \left\{ -\frac{1}{\tau_b} + \frac{1}{\tau_c} - \frac{\kappa}{\aleph} \times \mathrm{d}t \times \int_{\tilde{\lambda}} \left\{ \gamma_{\tilde{\lambda}} \times \frac{\phi(t,z,\tilde{\lambda})}{E_{\tilde{\lambda}}} \right. \right. \\ & \left. \left. \times \mu_{a,\mathrm{PpIX}}(t,z,\tilde{\lambda}) \right\} \mathrm{d}\tilde{\lambda} \right\}. \end{aligned} \tag{18}$$

From this new PpIX absorption coefficient, the new local total fluence rate, $\varphi(t_1,z,\lambda)$, is calculated. The process is

reiterated to calculate all the necessary PpIX absorption coefficients and local total fluence rates.

3.4 *Initialization*

According to the initial PpIX absorption coefficient, similarly to Liu et al.,[24] an initial exponential distribution of PpIX with depth, related to the progressive skin penetration of 5-ALA, is assumed

$$\mu_{a,\mathrm{PpIX}}(0,z,\lambda)=\mu_{a,\mathrm{PpIX}}(0{,}0,\lambda)\times\exp(-\eta z), \tag{19}$$

where η is the depth decay constant.

Moreover, from the above-mentioned relation $\mu_{a,\mathrm{PpIX}}(t,z,\lambda)=\varepsilon_{\mathrm{PpIX}}(\lambda)\times C_{\mathrm{PpIX}}(t,z)$, Eq. (19) becomes Eq. (20),

$$\mu_{a,\mathrm{PpIX}}(0,z,\lambda)=\varepsilon_{\mathrm{PpIX}}(\lambda)\times C_{\mathrm{PpIX}}(0{,}0)\times\exp(-\eta z). \tag{20}$$

3.5 *Parameters Specification*

The optical properties for epidermis are derived from the data obtained by Salomatina et al.[37] from normal human skin and the ones for actinic keratosis from the data reported in Garcia-Uribe et al.[38]

Regarding the time constant for the biological elimination of PpIX, denoted above as τ_b [Eq. (6)], we used the value of 1.29 h obtained by Star et al.[39] for normal human epidermis.

From the actinic keratosis data reported in Wiegell et al.,[22] the time constant for the conversion of 5-ALA into PpIX, τ_c [Eq. (7)], is deduced to be 1.1575 h, which is consistent with previously published values.[39,40]

Regarding the bimolecular rate constant, κ [Eq. (8)], we use the value of 5.3×10^9 l/mol/s reported in Ref. 41 as the bimolecular rate constant for quenching of protoporphyrin IX by a given conjugated fused tricyclic compound.

According to Wilkinson et al.[42] and Fernandez et al.,[43] the singlet oxygen quantum yield for PpIX, γ_λ [Eq. (11)], is set to 0.56 for all λ.

For the sake of consistency in Eq. (11) (the number of PpIX molecules in their singlet excited state cannot exceed the number of available PpIX molecules), the time increment, dt, is set to 1×10^{-5} s.

Based on the ratio of PpIX concentration at 0.2 mm to that on the surface of about 81% (respectively, 63%) obtained by Star et al.[39] for normal human epidermis after 3 h (respectively, 30 min) ALA administration, we deduce from Eq. (19) that the depth decay constant η is equal to 1.05/mm (respectively, 2.31/mm) for the red and blue light doses (respectively, for the daylight dose) with the above assumed 3 h (respectively, 30 min) incubation.

Regarding the initial concentration at the skin surface in Eq. 20, $C_{\mathrm{PpIX}}(0{,}0)$, we use the value 11.8 pmol/ml obtained by Smits et al.[44] from 11 patients with AK incubated with 20% ALA for 3 h. This value, which is suitable for the red and blue light doses with 3 h incubation, is not appropriate for the daylight dose with 30 min incubation. Based on a fluorescence intensity after 30 min incubation graphically deduced to be approximately 10 times lower than the one after 3 h incubation from Wiegell et al.[22] and Christiansen et al.,[45] we set the initial concentration at the skin surface for the daylight dose to 1.18 pmol/ml.

The PpIX molar extinction coefficients, $\{\varepsilon_{\mathrm{PpIX}}(\lambda)\}_\lambda$, are estimated from the PpIX absorption spectrum, $\{\mu_{a,\mathrm{PpIX,CRAN}}(\lambda)\}_\lambda$, measured by the Research Center for Automatic Control of Nancy (CRAN) from a PpIX concentration $C_{\mathrm{PpIX,CRAN}}$. The estimates, derived from the relation $\mu_{a,\mathrm{PpIX,CRAN}}(\lambda)=\varepsilon_{\mathrm{PpIX}}(\lambda)\times C_{\mathrm{PpIX,CRAN}}$, are deduced using the value of 1.24×10^5 l/mol/cm for ε(405 nm) reported in Natarajan et al.[46]

$$\varepsilon_{\mathrm{PpIX}}(\lambda)=\frac{\mu_{a,\mathrm{PpIX,CRAN}}(\lambda)}{C_{\mathrm{PpIX,CRAN}}}=\frac{\mu_{a,\mathrm{PpIX,CRAN}}(\lambda)}{\mu_{a,\mathrm{PpIX,CRAN}}(405\ \mathrm{nm})}\times\varepsilon_{\mathrm{PpIX}}(405\ \mathrm{nm}). \tag{21}$$

The published values for the model parameters that do not depend (respectively, that depend) on the light source are listed in Table 2 (respectively, in Table 3).

4 Applications

By down-sampling the skin model into Ω cuboids with $\mathrm{d}S=10\times10\ \mu\mathrm{m}^2$ and $\mathrm{d}z=10\ \mu$m as partially illustrated in Fig. 1, the photodynamic doses for each cuboid are computed for the three light doses according to Eq. (17).

We assume that, whatever the position in the AK of the skin sample model, the three obtained photodynamic doses are lethal for any cancer cells. It follows that the minimum of the three photodynamic doses at the deepest point of the AK, the darkest cuboid of the stack of cuboids shown in Fig. 1 that we denote by $\mathrm{PD}_{\mathrm{ref}}$, is also assumed to be lethal.

Based on the assumption that, whatever the light dose, a photodynamic dose equal to $\mathrm{PD}_{\mathrm{ref}}$ is sufficient to destroy any cancer cells, the treatment times and, therefore, the light doses required with the three light sources and their corresponding fluence rates reported in Table 1 to obtain a photodynamic dose equal to $\mathrm{PD}_{\mathrm{ref}}$ are computed.

All the computations were performed using a Matlab™ program on a standard personal computer (Intel Xeon CPU E3-1240 V2 3.40 GHz–8Go of RAM–Windows 7 64 bits).

5 Results

The photodynamic doses obtained in the skin sample model for the three different light doses are presented according to the central cross section of the skin sample model in Fig. 2 and along the above-defined central stack of cuboids (Fig. 1) in Fig. 3.

From Fig. 3, the depth evolution of the photodynamic doses for the red light dose (solid curve), the blue light dose (dashed curve) and the daylight dose (dotted curve) seems to be linear. With a slope of -1.76×10^4 from the linear regression, the depth evolution of the photodynamic dose for the daylight dose is approximately twice (respectively, 4.5 times) as rapid as the one for the blue light dose (respectively, the red light dose) with a slope of -8.89×10^3 (respectively, -3.89×10^3) (Fig. 3). From the last two slope values, the photodynamic dose for the blue light dose is found to decrease in depth approximately 2.3 times as fast as that of the red light dose.

Figure 4 shows the time evolution of the cumulative singlet oxygen produced at the deepest point of the AK for the three different light doses. This cumulative parameter was approximated at the above defined sampling times similarly to Eq. (17).

An exponential rise to a maximum $[f(t)=A\times[1-\exp(-t/\tau)]$, where A is the amplitude of the curve and

Table 2 Specification of the model parameters not depending on the light sources. For each reference, the photosensitizer and cells for which the values were obtained are reported in parentheses.

Parameters	Value	Reference (photosensitizer, cells)
Optical properties for epidermis		Salomatina et al.[37]
Optical properties for actinic keratosis		Garcia-Uribe et al.[38]
τ_b	1.3 h	Star et al.[39] (PpIX, normal human epidermis)
τ_c	1.1575 h	Wiegell et al.[22] (PpIX, actinic keratosis)
κ	5.3×10^9 l/mol/s	Bonda et al.[41] (PpIX)
γ_λ	0.56	Wilkinson et al.[42] (PpIX) Fernandez et al.[43] (PpIX)
dt	1×10^{-5} s	
ε (405 nm)	1.24×10^5 l/mol/cm	Natarajan et al.[46] (PpIX)

Table 3 Specification of the model parameters depending on the light sources. For each reference, the photosensitizer and cells for which the values were obtained are reported in parentheses.

Parameters	Light source	Value	Reference (photosensitizer, cells)
η	Red and blue light doses	1.05/mm	Star et al.[39] (PpIX, normal human epidermis)
	Daylight dose	2.31/mm	Star et al.[39] (PpIX, normal human epidermis)
$C_{\mathrm{PpIX}}(0,0)$	Red and blue light doses	11.8 pmol/ml	Smits et al.[44] (PpIX, actinic keratosis)
	Daylight dose	1.18 pmol/ml	Smits et al.[44] (PpIX, actinic keratosis) Wiegell et al.[22] (PpIX, actinic keratosis)

τ is the delay constant] was fit to each curve of Fig. 4. With a delay constant estimate of 746.73 s, the cumulative singlet oxygen produced for the blue light dose is found to increase about 1.3 times as fast as the one produced for the red light dose with a delay constant estimate of 985.65 s. With a delay constant estimate of 10356.57 s, the production rate of singlet oxygen for the daylight dose appears more than 10 times slower than those for the two others light doses.

From the three photodynamic doses of 5.67×10^6, 1.45×10^7, and 1.19×10^7 obtained at the deepest point of the AK with the red light dose, the blue light dose and the daylight dose, respectively (given by the last point of the curves in Figs. 3 and 4), the minimum one denoted $\mathrm{PD}_{\mathrm{ref}}$ was determined to be the red one.

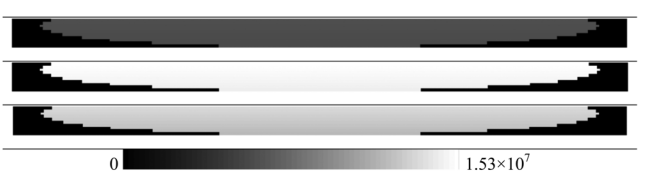

Fig. 2 Photodynamic doses in the central cross section of the skin sample model for the red light dose (row 1), the blue light dose (row 2) and the daylight dose (row 3). The doses are displayed, using the gray look-up table (row 4), in percent of the overall maximum photodynamic dose of 1.53×10^7 that was obtained at the skin surface with the blue light dose (see the y-intercept of the dashed curve in Fig. 3).

From Fig. 4, using the blue light with a fluence rate of 10 $\mathrm{mW/cm^2}$ (Table 1), a treatment time of about 254 s, which correspond to a light dose of 2.54 $\mathrm{J/cm^2}$, is required to obtain a photodynamic dose equal to $\mathrm{PD}_{\mathrm{ref}}$ at the deepest part in the AK. For the daylight dose (Table 1), a photodynamic

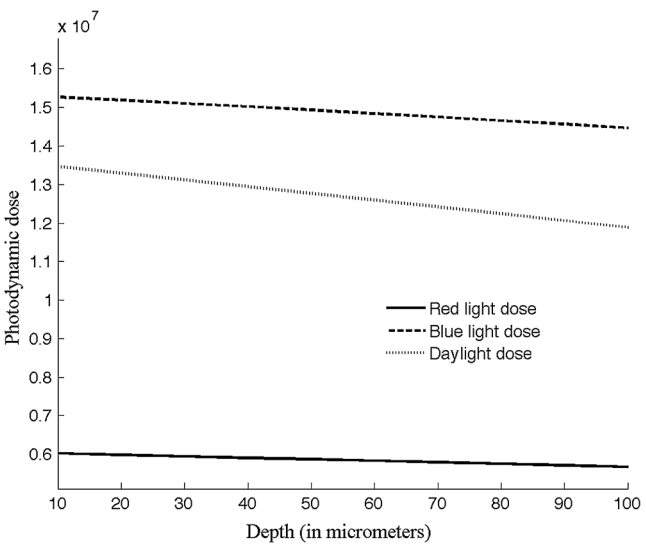

Fig. 3 Depth evolution of the photodynamic doses for the red light dose (solid curve), the blue light dose (dashed curve) and the daylight dose (dotted curve) along the central stack of cuboids of the skin sample model defined in Fig. 1.

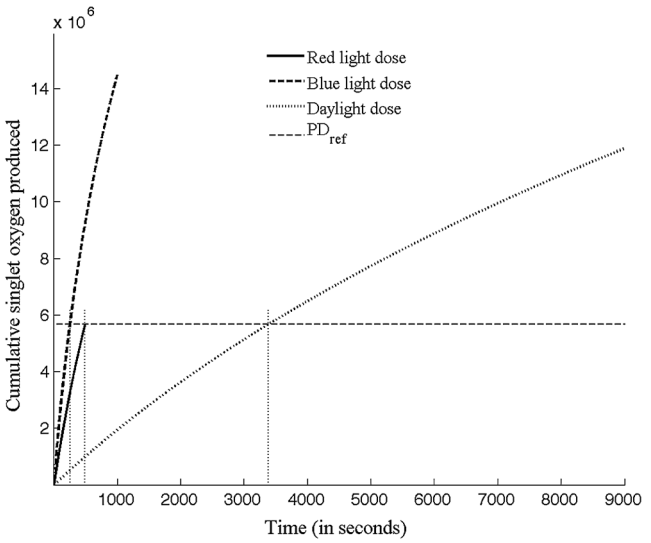

Fig. 4 Time evolution of the cumulative singlet oxygen produced for the red light dose (solid curve), the blue light dose (thick dashed curve) and the daylight dose (dotted curve) at the deepest point of the AK. The thin dashed line was used to determine the treatment times required with the blue light and the daylight as described in Table 1 to obtain a photodynamic dose at the deepest part of the AK equal to PD_{ref}.

dose equal to PD_{ref} is achieved at the deepest part of the AK using an exposure time of 3385 s.

Figure 5 shows examples of the evolution in time of the PpIX absorption coefficient obtained using the proposed model [Eq. (15)]. The corresponding evolutions in time of the PpIX absorption coefficient obtained by replacing the proposed model for photobleaching [Eq. (13)] by the common first order photobleaching model are also depicted in Fig. 5 for information purposes only. The exponential decay of the number of PpIX molecules assumed by the first order photobleaching model [Eq. (22)][23,28,35] leads to Eq. (23) in place of Eq. (15)

$$M_{\mathrm{PpIX},p}(t,z) = -\int_{\tilde{\lambda}} \beta_{\tilde{\lambda}} \times \phi(t,z,\tilde{\lambda}) \times M_{\mathrm{PpIX}}(t,z)\mathrm{d}\tilde{\lambda}, \qquad (22)$$

$$\mu_{a,\mathrm{PpIX}}(t+\mathrm{d}t,z,\lambda) = \mu_{a,\mathrm{PpIX}}(t,z,\lambda) + \mathrm{d}t \times \mu_{a,\mathrm{PpIX}}(t,z,\lambda) \times \left\{ -\frac{1}{\tau_b} + \frac{1}{\tau_c} - \int_{\tilde{\lambda}} \beta_{\tilde{\lambda}} \times \phi(t,z,\tilde{\lambda})\mathrm{d}\tilde{\lambda} \right\}, \qquad (23)$$

where the photobleaching dose constant parameters $\{\beta_{\tilde{\lambda}}\}_{\tilde{\lambda}}$ are set to 0.05 cm^2/J for all λ.[28]

From Fig. 5(b) (obtained for the 417 nm wavelength and the blue light dose), the time evolution curve obtained using the proposed model (solid curve) and the one obtained by considering the first order photobleaching model (dashed curve) follow somewhat similar trends. This similarity is not found for the 632 nm wavelength and the red light dose [Fig. 5(a)]. This may be explained by the use of a single value for all the photobleaching dose constant parameters $\{\beta_{\tilde{\lambda}}\}_{\tilde{\lambda}}$ that may be more appropriate for specific wavelengths. Furthermore, we can note a very rapid decrease of the dashed curve in Fig. 5(a), which presupposes a very (maybe too?) rapid consumption of PpIX.

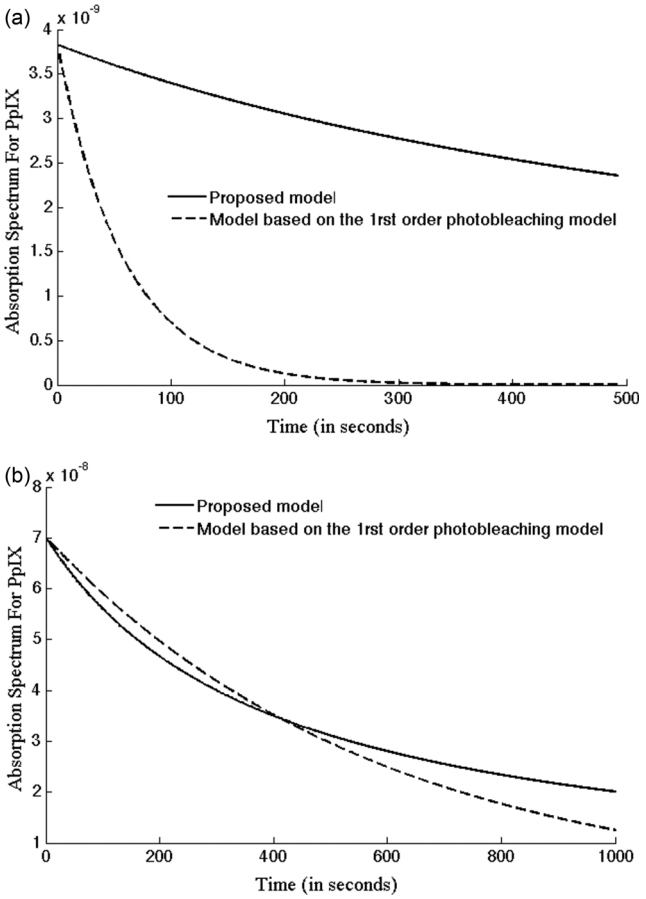

Fig. 5 Time evolution of the PpIX absorption coefficient at the deepest point of the AK obtained: (a) at wavelength 632 nm with the red light dose and (b) at wavelength 417 nm with the blue light dose (row 2). The solid curves represent the results obtained using the proposed model [Eq. (15)] while the dashed ones represent the results obtained by considering the first order photobleaching model [23,28,35] Eq. (23).

6 Discussion

In this paper, three light doses commonly used in the PDT treatment of actinic keratosis are compared using a mathematical modeling of the PDT process: the red light dose (632 nm, 37 $\mathrm{J/cm^2}$, 75 $\mathrm{mW/cm^2}$, 500 s),[30,31] the blue light dose (417 nm, 10 $\mathrm{J/cm^2}$, 10 $\mathrm{mW/cm^2}$, 1000 s),[33] and the daylight dose (9000 s,[22]) (Table 1).

The comparison is performed using a skin sample model consisting of an epidermis section with a thickness of 100 μm including an AK designed as a partial ellipsoid with a thickness of 150 μm (Fig. 1). Although similar high response rates have been reported for PDT treatment of AK using the three above introduced lights doses,[12,21,22,47] the deeper tissue penetration of red light compared to light with shorter wavelengths is known to make the red light dose more appropriate for the PDT treatment of thick lesions and deeper targets.[48] Nonetheless, regarding the thin actinic keratosis of the skin sample model used in this study, the blue light and the daylight can reasonably be assumed to allow sufficient tissue penetration to make the blue light and daylight doses efficient.

To perform the comparison of the three light doses, a photodynamic dose defined as the total cumulative singlet oxygen produced during treatment is introduced [Eqs. (16) and (17)]. This photodynamic dose depends on the local total fluence

rate which is obtained by the sum of the local diffuse fluence rate and the local incident fluence rate[28,29] [Eqs. (1)–(4)], and on the PpIX absorption coefficient. The three common kinds of changes in the PpIX absorption coefficient, namely the biological elimination of PpIX, the conversion of 5-ALA into PpIX and the photobleaching, are considered in the model [Eqs. (5)–(15)]. While usual exponential models are used for the biological elimination and the 5-ALA conversion, we proposed a new model for the photobleaching. The two commonly used models for photobleaching which are the first order photobleaching one in which PpIX is bleached exponentially by local total fluence rate[23,28] and the second order one using standard photochemical reaction kinetics[24,25] seem not to be appropriate for the present study. Regarding the first order photobleaching model, few published values are available for the involved photobleaching dose constant parameter and these values that are mainly obtained with a red light illumination[23,35] may not be suitable for the blue light and daylight illuminations and may, therefore, bias the comparison. The photobleaching model we proposed allows us to get rid of this photobleaching dose constant parameter and to make explicit the photobleaching dependence on wavelength [Eq. (13)]. Moreover it is adapted to the multispectral case and involves relatively few parameters compared to the complex second order photobleaching model.

The proposed model has been developed so as to involve only parameters for which empirical data are available and has required some assumptions and simplifications, especially in the change in the number of singlet oxygen molecules [Eqs. (9)–(12)]. These approximations are acceptable in the context of a comparison of light doses and may, in the current trends of low or blue dose, be suitable to define an experimental protocol to determine optimal treatment parameters.

All the parameters [Eqs. (1)–(20)] are set to published values, which were obtained with PpIX and with either normal human epidermis or AK (Table 2).

A first limitation of our model is the fact that the PpIX concentration is assumed to vary only with depth below the irradiated surface as in Ref. 28. Nonetheless, given the very small thickness of the skin sample model (100 μm), this assumption can be tolerated. A second limitation concerns the assumption of unlimited availability of oxygen (oxygen depletion due to photobleaching is not incorporated in the model). This assumption, made through the singlet oxygen quantum yield in Eq. (11), can be considered reasonable under light illumination with low fluence rates,[49,50] which is not the case for the red light dose. However, it is difficult to ascertain how the singlet oxygen quantum yield, γ_λ, would change during treatment and due to the lack of well-established empirical data and the variations of intrinsic parameters, constant γ_λ is usually assumed.[23] According to Ref. 51, this assumption does not seem to be inconsistent within the present study in which the skin sample model consists of an epidermis section with a thickness of 100 μm including an AK. In fact, Stücker et al.[51] have reported that the upper skin layers to a depth of 0.25 to 0.40 mm (including the epidermis layer) are almost exclusively supplied by diffused oxygen from the atmosphere, whereas the oxygen transport by blood capillaries extending to the upper layers of the dermis has a minor influence. It follows that the unlimited source of atmospheric oxygen allows unlimited oxygen availability in the skin sample model to be reasonably assumed.

Using red light and standard dose (fluence, 37 J/cm^2; fluence rate, 75 mW/cm^2; exposure time, 500 s[30,31]) a photodynamic dose of about 5.67×10^6 was obtained at the deepest part of the AK (i.e., at 95 μm from the skin surface). For a standard blue light dose (light dose, 10 J/cm^2; fluence rate, 10 mW/cm^2; exposure time, 1000 s[32,33]), a photodynamic dose of about 1.45×10^7 was estimated at the deepest part of the AK. With the daylight dose (exposure time, 9000 s[22,34]), a photodynamic dose of about 1.19×10^7 was obtained at the deepest part of the AK.

The minimum of these three photodynamic doses, which were considered as sufficiently lethal for AK cancer cells, was obtained with the red light dose (Fig. 4). The maximum of these three photodynamic doses was the blue one. This result can be explained by the small thickness of the tissue to be treated (100 μm) that makes the above mentioned deeper tissue penetration of red light compared to light with shorter wavelengths (illustrated by the lowest slope of the red line in Fig. 3) useless and illustrates the better match between the absorption spectrum of the PpIX and the blue light spectrum (PpIX has its largest absorption peak in the blue region). The daylight photodynamic dose was close to the blue one, which can be supported by the fact that all the PpIX absorption peaks are within the daylight spectrum.

The treatment time required with the blue light and a fluence rate of 10 mW/cm^2 (Table 1) to obtain a photodynamic dose equal to the red one at the deepest part of the AK was then estimated to be 254 s, which is equivalent to a quarter of the usual value of 1000 s.[30,31] This exposure time corresponds to a light dose of 2.54 J/cm^2. With daylight (Table 1), about 3385 s were required to obtain a photodynamic dose equivalent to the red one. A reduction of about 62% is found between the 3385 s and the 9000 s reported in Ref. 22. These results tend to highlight that the usual light doses (Table 1) are probably not well adapted and that the treatment parameters could be better determined to obtain a similar efficiency, but with an improved tolerability and a more manageable clinical practice (reduction in bed occupancy).

7 Conclusion

In this paper, we have proposed an original mathematical model for the photodynamic treatment of actinic keratosis. Applied with the three most common light doses reported in the literature, this model allows (1) a comparison of the local damage at the deepest part of the AK and (2) a comparison of the treatment times required to carry the same local damage to the deepest part of the AK to be made. These comparisons demonstrated that an optimization of the light doses parameters could lead to a similarly efficient and more suitable treatment.

Acknowledgments

The authors would like to thank A. N. Yaroslavsky from the Harvard Medical School, Massachusetts General Hospital, Wellman Center for Photomedicine, Boston, for providing the optical properties of epidermis used in this paper. The authors would like to thank A. Garcia-Uribe from the Department of Biomedical Engineering, Washington University in St. Louis, St. Louis, Missouri, and from the Department of Electrical and Computer Engineering, Texas A&M University, College Station, for granting access to the optical properties of actinic keratosis used in the experiments. The authors would like to thank C. Lavogiez from the Department of Dermatology, University Hospital, Lille, France, for her cooperation in this study.

References

1. A. P. Castano, T. N. Demidova, and M. R. Hamblin, "Mechanisms in photodynamic therapy: part one—photosensitizers, photochemistry and cellular localization," *Photodiagn. Photodyn. Ther.* **1**(4), 279–293 (2004).
2. K. Plaetzer et al., "Photophysics and photochemistry of photodynamic therapy: fundamental aspects," *Lasers Med. Sci.* **24**(2), 259–268 (2009).
3. C. A. Morton et al., "Guidelines for topical photodynamic therapy: report of a workshop of the British Photodermatology Group," *Br. J. Dermatol.* **146**(4), 552–567 (2002).
4. R. Bissonette, A. Bergeron, and Y. Liu, "Large surface photodynamic therapy with aminolevulinic acid: treatment of actinic keratoses and beyond," *J. Drugs Dermatol.* **3**(Suppl. 1), S26–S31 (2004).
5. L. R. Braathen et al., "Guidelines on the use of photodynamic therapy for nonmelanoma skin cancer: an international consensus," *J. Am. Acad. Dermatol.* **56**(1), 125–143 (2007).
6. C. A. Morton, K. E. McKenna, and L. E. Rhodes, "Guidelines for topical photodynamic therapy: update," *Br. J. Dermatol.* **159**(6), 1245–1266 (2008).
7. S. R. Wiegell, "Update on photodynamic treatment for actinic keratosis," *Curr. Probl. Dermatol.* **46**, 122–128 (2015).
8. J. C. Kennedy, R. H. Pottier, and D. C. Pross, "Photodynamic therapy with endogenous protoporphyrin IX: basic principles and present clinical experience," *J. Photochem. Photobiol. B* **6**(1–2), 143–148 (1990).
9. Q. Peng et al., "5-Aminolevulinic acid-based photodynamic therapy. Clinical research and future challenges," *Cancer* **79**(12), 2282–2308 (1997).
10. C. A. Morton et al., "European guidelines for topical photodynamic therapy part 1: treatment delivery and current indications–actinic keratoses, Bowen's disease, basal cell carcinoma," *J. Eur. Acad. Dermatol. Venereol.* **27**(5), 536–544 (2013).
11. D. J. Piacquadio et al., "Photodynamic therapy with aminolevulinic acid topical solution and visible blue light in the treatment of multiple actinic keratoses of the face and scalp," *Arch. Dermatol.* **140**(1), 41–46 (2004).
12. C. Morton et al., "Intraindividual, right-left comparison of topical methyl aminolaevulinate-photodynamic therapy and cryotherapy in subjects with actinic keratoses: a multicentre, randomized controlled study," *Br. J. Dermatol.* **155**(5), 1029–1036 (2006).
13. C. A. Morton et al., "Comparison of photodynamic therapy with cryotherapy in the treatment of Bowen's disease," *Br. J. Dermatol.* **135**(5), 766–771 (1996).
14. P. G. Calzavara-Pinton et al., "Methylaminolaevulinate-based photodynamic therapy of Bowen's disease and squamous cell carcinoma," *Br. J. Dermatol.* **159**(1), 137–144 (2008).
15. N. Basset-Seguin et al., "Topical methyl aminolaevulinate photodynamic therapy versus cryotherapy for superficial basal cell carcinoma: a 5 year randomized trial," *Eur. J. Dermatol.* **18**(5), 547–553 (2008).
16. R. M. Szeimies et al., "A clinical study comparing methyl aminolevulinate photodynamic therapy and surgery in small superficial basal cell carcinoma (8–20 mm), with a 12-month follow-up," *J. Eur. Acad. Dermatol. Venereol.* **22**(11), 1302–1311 (2008).
17. J. Tyrrell, S. M. Campbell, and A. Curnow, "The effect of air cooling pain relief on protoporphyrin IX photobleaching and clinical efficacy during dermatological photodynamic therapy," *J. Photochem. Photobiol.* **103**(1), 1–7 (2011).
18. K. Z. Stangeland and S. Kroon, "Cold air analgesia as pain reduction during photodynamic therapy of actinic keratoses," *J. Eur. Acad. Dermatol. Venereol.* **26**(7), 849–854 (2012).
19. A. H. Arits et al., "Pain during topical photodynamic therapy: uncomfortable and unpredictable," *J. Eur. Acad. Dermatol. Venereol.* **24**(12), 1452–1457 (2010).
20. Z. Apalla et al., "The impact of different fluence rates on pain and clinical outcome in patients with actinic keratoses treated with photodynamic therapy," *Photodermatol. Photoimmunol. Photomed.* **27**(4), 181–185 (2011).
21. E. H. Tschen et al., "Photodynamic therapy using aminolaevulinic acid for patients with nonhyperkeratotic actinic keratoses of the face and scalp: phase IV multicentre clinical trial with 12-month follow up," *Br. J. Dermatol.* **155**(6), 1262–1269 (2006).
22. S. R. Wiegell et al., "Continuous activation of PpIX by daylight is as effective as and less painful than conventional photodynamic therapy for actinic keratoses; a randomized, controlled, single-blinded study," *Br. J. Dermatol.* **158**(4), 740–746 (2008).
23. R. M. Valentine et al., "Monte Carlo modeling of in vivo protoporphyrin IX fluorescence and singlet oxygen production during photodynamic therapy for patients presenting with superficial basal cell carcinomas," *J. Biomed. Opt.* **16**(4), 048002 (2011).
24. B. Liu, T. J. Farrell, and M. S. Patterson, "A dynamic model for ALA-PDT of skin: simulation of temporal and spatial distributions of ground-state oxygen," *Phys. Med. Biol.* **55**(19), 5913–5932 (2010).
25. B. Liu, T. J. Farrell, and M. S. Patterson, "Comparison of noninvasive photodynamic therapy dosimetry methods using a dynamic model of ALA-PDT of human skin," *Phys. Med. Biol.* **57**, 825–841 (2012).
26. Y. Wang et al., "Choosing optimal wavelength for photodynamic therapy of port wine stains by mathematic simulation," *J. Biomed. Opt.* **16**(9), 098001 (2011).
27. G. Hennig, H. Stepp, and A. Johansson, "Photobleaching-based method to individualize irradiation time during interstitial 5-aminolevulinic acid photodynamic therapy," *Photodiagn. Photodyn. Ther.* **8**(3), 275–281 (2011).
28. T. J. Farrell et al., "Modeling of photosensitizer fluorescence emission and photobleaching for photodynamic therapy dosimetry," *Appl. Opt.* **37**(31), 7168–7183 (1998).
29. S. A. Carp, S. A. Prahl, and V. Venugopalan, "Radiative transport in the delta-P1 approximation: accuracy of fluence rate and optical penetration depth predictions in turbid semi-infinite media," *J. Biomed. Opt.* **9**(3), 632–647 (2004).
30. H. Moseley, "Light distribution and calibration of commercial PDT LED arrays," *Photochem. Photobiol. Sci.* **4**, 911–914 (2005).
31. J. Tyrrell, S. M. Campbell, and A. Curnow, "Protoporphyrin IX photobleaching during the light irradiation phase of standard dermatological methyl-aminolevulinate photodynamic therapy," *Photodiagn. Photodyn. Ther.* **7**, 232–238 (2010).
32. DUSA Pharmaceuticals, "Levulan Kerastick topical solution 20%," Package insert, http://www.dusapharma.com (7 June 2009).
33. C. B. Warren, S. Lohser, and L. C. Wen, "Noninvasive fluorescence monitoring of protoporphyrin IX production and clinical outcomes in actinic keratoses following short-contact application of 5-aminolevulinate," *J. Biomed. Opt.* **15**(5), 051607 (2010).
34. C Honsberg and S Bowden, PVCDROM, 2014, http://www.pveducation.org/pvcdrom/appendices/standard-solar-spectra.
35. C. L. Campbell et al., "Mathematical modeling of daylight activated photodynamic therapy for continuous accumulation of, PpIX," in *Proc. Laser Europe Conf.* (2014).
36. J. S. Dysart, G. Singh, and M. S. Patterson, "Calculation of singlet oxygen dose from photosensitizer fluorescence and photobleaching during mTHPC photodynamic therapy of MLL cells," *Photochem. Photobiol.* **81**, 196–205 (2005).
37. E. Salomatina et al., "Optical properties of normal and cancerous human skin in the visible and near-infrared spectral range," *J. Biomed. Opt.* **11**(6), 064026 (2006).
38. A. Garcia-Uribe et al., "In vivo diagnosis of melanoma and nonmelanoma skin cancer using oblique incidence diffuse reflectance spectrometry," *Cancer Res.* **72**(11), 2738–2745 (2012).
39. W. M. Star et al., "Quantitative model calculation of the time-dependent protoporphyrin IX concentration in normal human epidermis after delivery of ALA by passive topical application or iontophoresis," *Photochem. Photobiol.* **75**(4) 424 (2002).
40. E. Angell-Petersen et al., "Porphyrin formation in actinic keratosis and basal cell carcinoma after topical application of methyl 5-aminolevulinate," *J. Invest. Dermatol.* **126**, 265–271 (2006).
41. C. A. Bonda and S. Hu, "Tricyclic energy quencher compounds for reducing singlet oxygen generation," Patent WO2014025370 A1 (2014).
42. F. Wilkinson, W. P. Helman, and A. B. Ross, "Quantum yields for the photosensitized formation of the lowest electronically excited singlet state of molecular oxygen in solution," *J. Phys. Chem. Ref. Data* **22**, 113–262 (1993).
43. J. M. Fernandez, M. D. Bilgin, and L. I. Grossweiner, "Singlet oxygen generation by photodynamic agents," *J. Photochem. Photobiol. B* **37**(1), 131–140 (1997).

44. T. Smits and A. C. E. Moor, "New aspects in photodynamic therapy of actinic keratoses," *J. Photochem. Photobiol.* **96**(3), 159–169 (2009).
45. K. Christiansen, P. Bjerring, and A. Troilius, "5-ALA for photodynamic photorejuvenation-optimization of treatment regime based on normal-skin fluorescence measurements," *Lasers Surg. Med.* **39**, 302–310 (2007).
46. P. Natarajan and C. Raja, "Studies on interpolymer self-organisation behaviour of protoporphyrin IX bound poly(carboxylic acid)s with complimentary polymers by means of fluorescence techniques," *Eur. Polym. J.* **40**, 2291–2303 (2004).
47. R. M. Szeimies et al., "Topical methyl aminolevulinate photodynamic therapy using red light-emitting diode light for multiple actinic keratoses: a randomized study," *Dermatol. Surg.* **35**(4), 586–592 (2009).
48. M. T. Wan and J. Y. Lin, "Current evidence and applications of photodynamic therapy in dermatology," *Clin. Cosmet. Investig. Dermatol.* **21**(7), 145–163 (2014).
49. J. H. Woodhams, A. J. Macrobert, and S. G. Bown, "The role of oxygen monitoring during photodynamic therapy and its potential for treatment dosimetry," *Photochem. Photobiol. Sci.* **6**(12), 1246–1256 (2007).
50. K. Langmack et al., "Topical photodynamic therapy at low fluence rates-theory and practice," *J. Photochem. Photobiol. B* **60**(1), 37–43 (2001).
51. M. Stücker et al., "The cutaneous uptake of atmospheric oxygen contributes significantly to the oxygen supply of human dermis and epidermis," *J. Physiol.* **538**(3), 985–994 (2002).

Anne-Sophie Vignion-Dewalle is a research engineer—expert in scientific computing at the French National Institute of Health and Medical Research (INSERM) unit 1189 Image Assisted Laser Therapies Assisted for Oncology. Her research activity is mainly focused on laser therapies and more specifically on the modeling of the photodynamic therapy process.

Nacim Betrouni is a research scientist at the French National Institute of Health and Medical Research (INSERM) in the U1189 (Image Assisted Laser Therapies Assisted for Oncology) laboratory. His research topics concern optimization of image guided laser procedures, including thermal and photodynamic therapies.

Jean-Baptiste Tylcz is obtained his PhD in automatic control from University of Lorraine. His research focuses on the system identification and control of biological systems. During his PhD at the Automatic Control Research Centre of Nancy (CRAN), he developed a device controlling the cytotoxic phase of photodynamic therapy (PDT). He is currently occupying a postdoctoral position at the INSERM in the U1189 and works on fluorescence uses to improve PDT.

Maximilien Vermandel has a master's degree and a PhD in automatic and signal processing from University of Sciences and Technologies of Lille, and a master's degree in medical physics from University Paul Sabatier of Toulouse. Currently, he is associate professor at the University of Lille and Medical Physicist at the Lille University Hospital. Its research topics aim to develop image guided photodynamic therapy dedicated to neurosurgery, especially high-grade glioma management.

Laurent Mortier is dermatologist at University Hospital of Lille, France, and a member of the INSERM in the U1189 Image Assisted Laser Therapies Assisted for Oncology. His clinical and research interests include the use of photodynamic therapy in dermatology: treatment of skin conditions and antimicrobial photodynamic therapy.

Serge Mordon is the director of INSERM in the U1189 (Image Assisted Laser Therapies Assisted for Oncology). His research is mainly focused on focal laser ablation and photodynamic therapy. He is the author of sixteen issued patents and 400 peer-reviewed papers. He is a board member of several professional societies. He is an associate editor of the journal *Lasers in Surgery and Medicine*. In 2015, he has been nominated for Finland Distinguished Professor.